Application of fragment-based drug discovery to membrane proteins

Früh, V.

Chapter

5

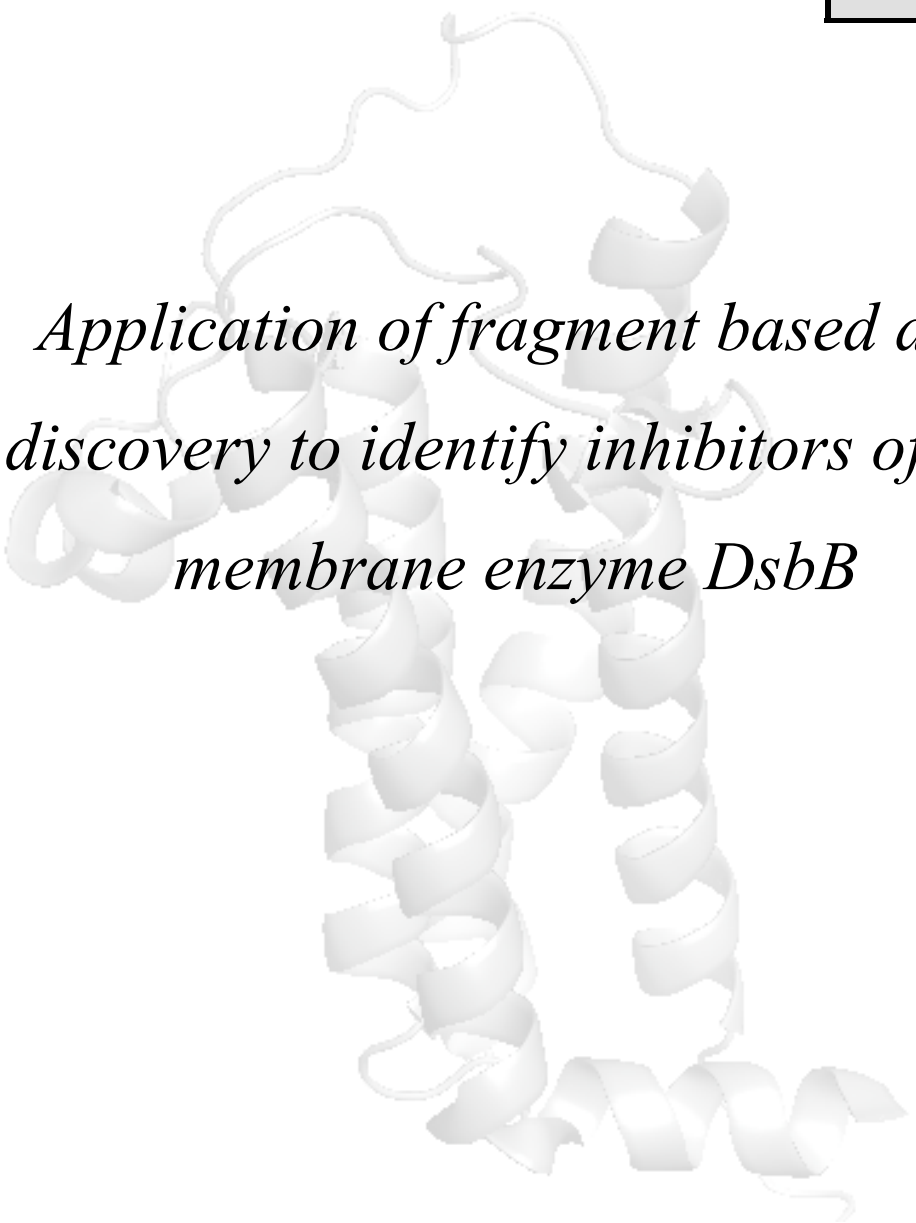

Application of fragment based drug discovery to identify inhibitors of the membrane enzyme DsbB

Membrane proteins are an interesting class due to the variety of cellular functions and their importance as pharmaceutical targets, but they pose significant challenges for fragment based drug discovery approaches. Here we present the first successful use of biophysical methods to screen for fragment ligands to an integral membrane protein. Using the recently developed Target Immobilized NMR Screening approach, we screened 1,200 fragments for binding to the enzyme Disulphide bond forming protein B. Biochemical and biophysical validation of the 8 most potent hits revealed an IC_{50} range of 7 to 200 μM, which could be categorized as cofactor binding inhibitors or mixed model inhibitors of both cofactor and substrate protein interaction. Our results clearly establish the utility of fragment based methods in the development of inhibitors of membrane proteins, making a wide variety of important membrane bound pharmaceutical targets amenable to such an approach.

This chapter has been recently submitted as a manuscript: Virginie Früh, Yunpeng Zhou, Caroline Loch, Eiso AB, Herman Verheij, John H. Bushweller and Gregg Siegal. Application of Fragment Based Drug Discovery to Identify Inhibitors of the Integral Membrane Enzyme DsbB.
Nature Chemical Biology. Accepted for review 2009.

With 60 % of currently marketed drugs targeting membrane proteins[36], it is clear that finding small molecules to modulate the function of such proteins is essential. High throughput screening (HTS) methods have been successful in identifying such compounds, but because the methods of detection rely on functional assays, they are generally only sensitive to submicromolar interactions. Such relatively tight interactions are generally only observed for larger compounds (300 - 500 Da). However, it has proved challenging to simultaneously optimize potency and absorption, distribution, metabolism, and excretion (ADME) properties of these "lead-like" or "drug-like" compounds. Furthermore, such large compounds inefficiently explore the binding sites of proteins[17]. Fragment-based drug discovery (FBDD) has become a powerful complementary approach to HTS for generating novel chemical modulators of pharmaceutical targets. FBDD screens small libraries (1,000 - 20,000 compounds) of so-called drug "fragments" that are typically described by a "rule of threes"[15] (Ro3, M_r < 300 Da, cLogP < 3, H-bond donors < 3, H-bond acceptors < 3, number of rotatable bonds < 3 and TPSA (total polar surface area) < 60 Å^2) for binding to the target. Ro3 compliant compounds typically bind the target with K_d greater than 10 μM. In order to detect such weak binding, sensitive biophysical techniques are required. Commonly used techniques for detecting fragment binding include NMR, X-ray crystallography and surface plasmon resonance (SPR)[207]. Although these methods have been successfully applied to an array of soluble protein targets[239], they have failed in one way or another when applied to membrane proteins. There are two primary reasons for this failure: insufficient quantity of the target and non-specific binding of compounds to the solubilization media. Since many biophysical methods require tens or even hundreds of mg of protein and most membrane proteins are difficult to produce in even single mg quantities, many potential applications of FBDD to membrane proteins have been impractical. For those membrane proteins that can be produced in sufficient quantity, non-specific partitioning of fragments into the detergent micelle or lipid bilayer used to solubilize the protein has been a severe and limiting problem.

We have developed an NMR-based fragment screening approach which has proven, in principle, capable of overcoming the challenges posed by membrane proteins[23] (Chapter 4). The approach, called Target Immobilized NMR Screening (TINS)[77], involves immobilizing a target

and a reference protein in two compartments of a dual-cell sample holder[205] and simultaneously injecting mixtures of fragments in an automated process. For each mixture a 1D, spatially selective ^{1}H NMR spectrum, which only contains contributions from the fragments in solution, is recorded. Fragment binding to the target protein is readily detected by the decrease in peak amplitude resulting from the greatly enhanced transverse relaxation experienced in the bound state. The reference protein, which is selected for minimal specific small molecule binding, serves to cancel out non-specific binding of fragments to protein surfaces. Hits can therefore be easily detected by comparing spectra recorded in the presence of the target to those recorded in the presence of the reference. By repeatedly using the same sample to screen the entire fragment collection (~1,500 compounds) typically only ~25 - 50 nmol of protein is required. Furthermore, the reference system is expected to account for non-specific binding of fragments to the detergent micelles in which the membrane proteins are solubilized. We therefore sought to apply TINS to a *bona fide*, integral membrane pharmaceutical target.

The inner membrane protein of *E. coli* Disulphide bond forming protein B (DsbB), and its homologs in other gram-negative bacteria, is an oxidoreductase that is essential for protein disulfide bond formation in the periplasm. Periplasmic DsbA functions as the catalyst for protein disulfide bond formation and is reoxidized by DsbB with concomitant reduction of bound ubiquinone or menaquinone. Since many bacterial virulence factors are secreted proteins that require disulfide bonds for proper folding and function, the DsbA/DsbB system is a potential antimicrobial drug target[94,240,241]. DsbB is an ideal candidate to test the TINS methodology since it can be readily produced and solubilized in detergent micelles where it retains a robust enzymatic activity which is easily assayed. In addition, a wealth of biochemical data is available that describes the enzymatic activity of the wildtype as well as numerous relevant mutants[242,243,244,245]. Finally, the 3D structures of the wildtype DsbB bound to its redox partner DsbA[92] and of a mutant representing an enzymatic intermediate are available[62]. Selection of an appropriate reference protein is critical to insure the robust performance of TINS. Our previous experience using the *E. coli* Outer membrane protein A (OmpA) transmembrane domain, which has native structure under the same detergent micelle conditions as DsbB, in a limited screen of

about 200 compounds, suggested that it had minimal small molecule binding[23] (Chapter 4). Thus we have utilized OmpA as a reference protein.

Here we report the first complete screen of a fragment library against an integral membrane protein. Hits from the screen have been validated and characterized with respect to mode of action using an enzyme inhibition assay. Finally, the binding mode of two classes of inhibitors has been investigated by analysis of chemical shift perturbations induced upon fragment binding to isotope labelled, mutant DsbB.

Methods

Protein immobilization

DsbA, DsbB, and OmpA were expressed and purified as previously reported[1,79,99]. The Actigel ALD resin (Sterogene, Carlsbad, CA, USA), available commercially, was used as a 50 % slurry and all experiments were carried out at 4 ºC when possible. The resin was washed with cold phosphate buffer (50 mM Na_2HPO_4, 50 mM KH_2HPO_4, 100 mM NaCl) at pH 7.5. 200 nmol of DPC solubilized DsbB was added to 1 ml bed volume of resin. The reductant sodium cyanoborohydride ($NaCNBH_3$) was added to a final concentration of 0.1 M. After an overnight incubation at 4 °C, residual unreacted aldehydes were blocked by addition of 50 mM Tris buffer and $NaCNBH_3$ for another 2 hours. The same procedure was repeated for DPC solubilized OmpA. Quantification of immobilized protein was monitored by absorption of the supernatant at 280 nm before and after immobilization, and by SDS-page gel with a known standard curve and volume analysis. This data indicated that a final concentration of 100 μM of both immobilized DsbB and OmpA was achieved, equating to a 50 % yield.

DsbB activity assays

DsbB activity was quantified by measuring the capacity of the enzyme to reoxidize the protein DsbA or reduce its cofactor Ubiquinone-5, also called Coenzyme Q1 (UQ1) at pH 6.2. DsbA

was reduced with 10 mM DTT for 10 minutes on ice. DTT was subsequently removed by gel filtration on a PD-10 column pre-equilibrated with degassed distilled water containing 0.1 mM EDTA. EDTA was used to chelate metal ions which would otherwise give rise to spurious reoxidation of DsbA[244]. DsbA fluorescence (excitation at 295 nm and emission at 330 nm) was measured in the presence of DsbB and UQ1 in 50 mM sodium phosphate, 100 mM NaCl, 0.1 % detergent (DPC or DDM depending on which was used to solubilize DsbB) and 0.1mM EDTA) at 30 ºC. The activity of DsbB in terms of moles ubiquinone reduced/moles DsbB min^{-1} could be calculated by using the initial slope of fluorescence decrease upon DsbA oxidation, or by using the slope of absorption decrease at 275 nm upon reduction of UQ1[99].

To measure activity of immobilized DPC solubilized DsbB, resin was aliquoted and diluted with degassed activity assay buffer to a final protein concentration of approximately 20 nM. For an appropriate baseline, an equivalent amount of resin without protein (blank resin) was prepared in the same manner. Quinone reduction was monitored in both samples after addition of 20 μM coenzyme Q1 and 20 μM DsbA.

Target Immobilized NMR Screening

Immobilized, DPC solubilized DsbB and OmpA were each packed into a separate cell of a dual-cell sample holder[205]. The cell was attached to a Gilson 210 autosampler *via* capillary tubing and inserted into an 8 mm, ^{1}H selective, flow-injection probe in a 500 MHz magnet. Mixes of the 1,270 fragments were made by 200 fold dilution of a 100 mM stock of each compound in d_6-DMSO such that the final DMSO concentration was never greater than 5 %. Upon injection of each mix into the dual-cell sample holder, flow was stopped and spatially selective Hadamard spectroscopy[206] was used to acquire a 1D ^{1}H spectrum of each sample separately. A CPMG T2 filter of 80 ms was used to remove residual broad resonances from the sepharose resin. The cycle time was about 35 minutes, with 30 minutes required for the NMR experiment and 5 for sample handling, resulting in a total time of about 5 days to complete the screen. To maintain proper fold of each protein, 5 mM deuterated DPC was included in the buffer (20 mM phosphate buffer in D_2O, 100 mM NaCl, pH 7.6) used to wash the fragment mixes from

the sample holder. Scaling of peak intensities and positions between the two cells during data analysis was facilitated by adding glycine and TSP in all fragment mixes.

Biochemical hit validation

All fragments from the screen that were designated as positive for binding were assayed for DsbB inhibition at 250 μM. The amount of DMSO in all biochemical assay controls was adjusted to match the amount present when fragments were tested. Those compounds that showed more than 70 % inhibition at 250 μM were further characterized by titration from 0.0001 mM to 10 mM to generate IC_{50} curves. The mode of action for the 8 most potent fragments was determined from competition enzyme assays. For this analysis either DsbA or UQ1 was titrated in from 0.2 to 40 μM, while the other was kept constant at 40 μM. For each titration point, slopes were measured in the presence of 5, 10, and 75 μM of the fragment. DsbB activity data was analyzed using the non-linear regression curve fitting routines in Graph Pad Prism v. 5.01 (Graph Pad, San Diego, CA, U.S.A.). Statistical significance was evaluated with the student's T-test. Depending on the light absorbing properties of the fragments, they were used in either the fluorescence or UV-absorbance assay. Compounds which were not compatible with the assays due to high intrinsic fluorescence, high UV absorbance or irregular baselines were not included in the analysis.

Biophysical hit validation

Due to the poor quality of the NMR spectra of the wild-type DsbB, it was necessary to use a mutant that represents an intermediate in the disulfide oxidation pathway[62]. Accordingly, validated hits from the screen were titrated at 1, 5, and 10 mM into ^{15}N-labelled DsbB[CSSC] mutant (C44S, C104S). [^{15}N,^{1}H] HSQC experiments were acquired at 40 ºC in a Bruker DRX 600 MHz spectrometer equipped with a cryoprobe. A reference titration of DMSO and a non-binding fragment from the screen were used to subtract chemical shift perturbations not related to fragment binding.

RESULTS

Structure of a micelle solubilized DsbB disulfide intermediate

We have previously reported the solution structure of a mutated form of DsbB in which cysteines 44 and 104 have been mutated to serine, resulting in a stable disulfide bridge between Cys41 and Cys130 in DPC micelles (referred to as DsbB[CSSC], Figure 1)[62].

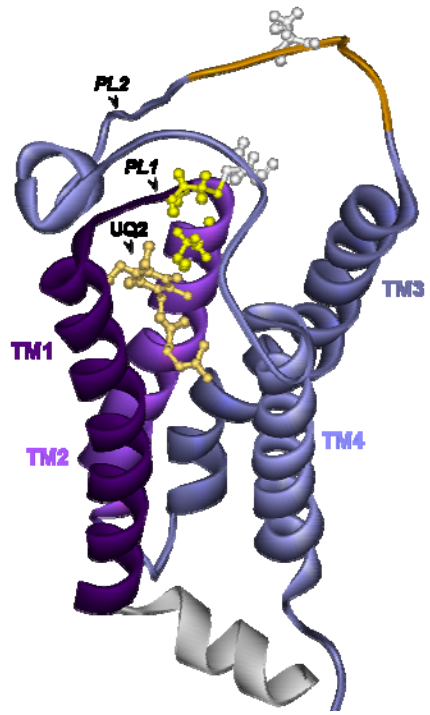

Figure 1. Solution NMR structure of DsbB[CSSC] (PDB 2K74), viewed approximately parallel to the membrane plane. The upper surface faces the periplasm while the lower surface faces the cytoplasm. DsbB has four transmembrane helices (TM 1 - 4) and an N-terminal cytoplasmic amphipathic helix (H1). The functionally important second periplasmic loop is divided into two parts (PL2 and PL2') by a short horizontal helix (H2). The four essential Cys residues (yellow) are located at the N-terminus of TM2 and in PL2 and PL2'. The binding site for the ubiquinone cofactor (black and red) lies on the periplasmic side of DsbB and is formed by TM1, TM2 and TM4. Two regions in PL2 and PL2' that form the DsbA binding site are colored red.

This form of the protein, with a disulfide bridge between periplasmic loops 1 and 2, is an intermediate in the redox reaction that results in transfer of electrons from DsbA to a ubiquinone buried in DsbB[246]. The N-terminus of micelle solubilized DsbB[CSSC] forms an amphipathic helix that runs parallel to the cytoplasmic side of the inner membrane. The ubiquinone binding site is near the periplasmic side of the inner membrane with the isoprenoid tail extending down the groove between TM1 and TM4. The interloop disulfide between Cys41 and Cys130 is approximately 7.5 Å from the benzoquinone ring.

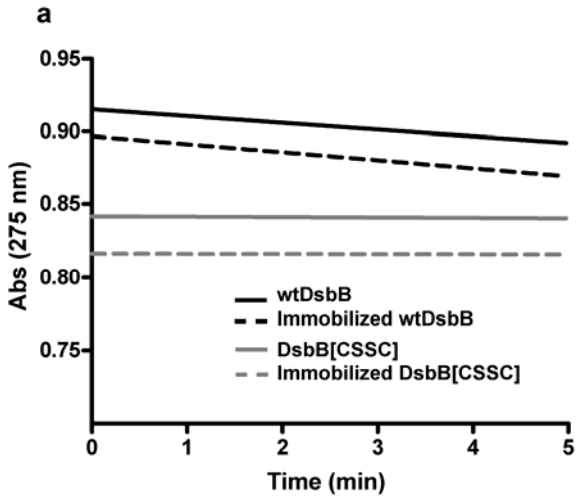

b

Enzyme	K_{cat} (M UQ1/ M DsbB-min^{-1})
DsbB wt	267 ± 14
DsbB wt (immobilized)	238 ± 27
DsbB[CSSC]	13 ± 2
DsbB[CSSC] (immobilized)	10 ± 1
DsbB wt*	278

Figure 2: Enzymatic activity of wildtype DsbB (wt) and DsbB[CSSC] in solution and immobilized. Both forms of DsbB were assayed at 5 nM. The graph shows the reduction of UQ1 observed by a decrease in absorption at 275 nm (**a**). The calculated K_{cat} values for each form of DsbB are compared with literature values *[1] (**b**).

DsbB functional immobilization and enzymatic activity

Wildtype DsbB (containing endogenous quinone), solubilized in DPC micelles, was immobilized on a Sepharose resin containing a 6 atom hydrophilic linker terminating in an aldehyde *via* a Schiff's base intermediate. At the pH selected (7.4), this reaction is relatively specific for the free N-terminus. A final concentration of approximately 100 μM DsbB (nmol protein per ml settled bed volume) was readily achieved. The functionality of the immobilized enzyme was compared to non-immobilized, micelle solubilized enzyme. Figure 2 shows that immobilized wildtype DsbB retained 90 % activity in comparison to the non-immobilized protein and that the K_{cat} of both forms of the protein was close to values previously reported[1].

DsbB[CSSC] was assayed for enzymatic activity in both immobilized and non-immobilized forms and, as expected, had no activity (Figure 2)[1,62,245]. The ready immobilization with retention of enzymatic activity suggests that the N-terminus of DsbB is accessible in the micelle solubilized protein. Given the success of the immobilization strategy with DsbB, we used the same approach with OmpA which had also been solubilized in DPC micelles. We observed a similar yield of OmpA immobilization. Since OmpA has no enzymatic activity, we had to assume that its structure was not grossly perturbed by the immobilization process. Independent

experiments showed that immobilized samples of DsbB were stable for at least one month after storage at 4 ºC (data not shown).

Target immobilized NMR Screening (TINS)

In order to screen our fragment collection, DsbB and OmpA were immobilized at a solution equivalent of 100 μM and separately packed into cells of the dual-cell sample holder[205].

Preliminary studies clearly demonstrated that repeated cycles of compound application and washing in the absence of added detergent resulted in rapid degradation of DsbB activity, as would be expected of a membrane protein[23] (Chapter 4). Therefore deuterated DPC was included at a minimum concentration of 5 mM (5 x critical micellar concentration) in the buffer used to wash the compounds from the sample holder. To monitor the integrity of the DsbB sample during the screen, the binding of synthetic UQ1 was observed. The TINS effect, defined as the average ratio of the amplitude of peaks in the presence of DsbB to that in the presence of OmpA, remained constant for UQ1 throughout the screen[23]. This fact suggests that either the bound quinone was not cumulatively displaced or leached from the DsbB or that the injected UQ1 was sufficient to replace any lost quinone. A total of 1200 fragments, in 182 mixtures containing 3 - 9 fragments at 500 μM each, were assayed for binding to DsbB. A spatially selective Hadamard NMR experiment[206] was used to simultaneously acquire a 1D ^{1}H spectrum of compounds in the presence of DsbB or OmpA. The data resulting from the screen could be analysed directly without deconvolution because fragments could be directly identified by comparing peaks from TINS spectra with the fragment's individual reference spectra (Figure 3). The ready identification of binders enabled a totally automated analysis of the complete screening data,

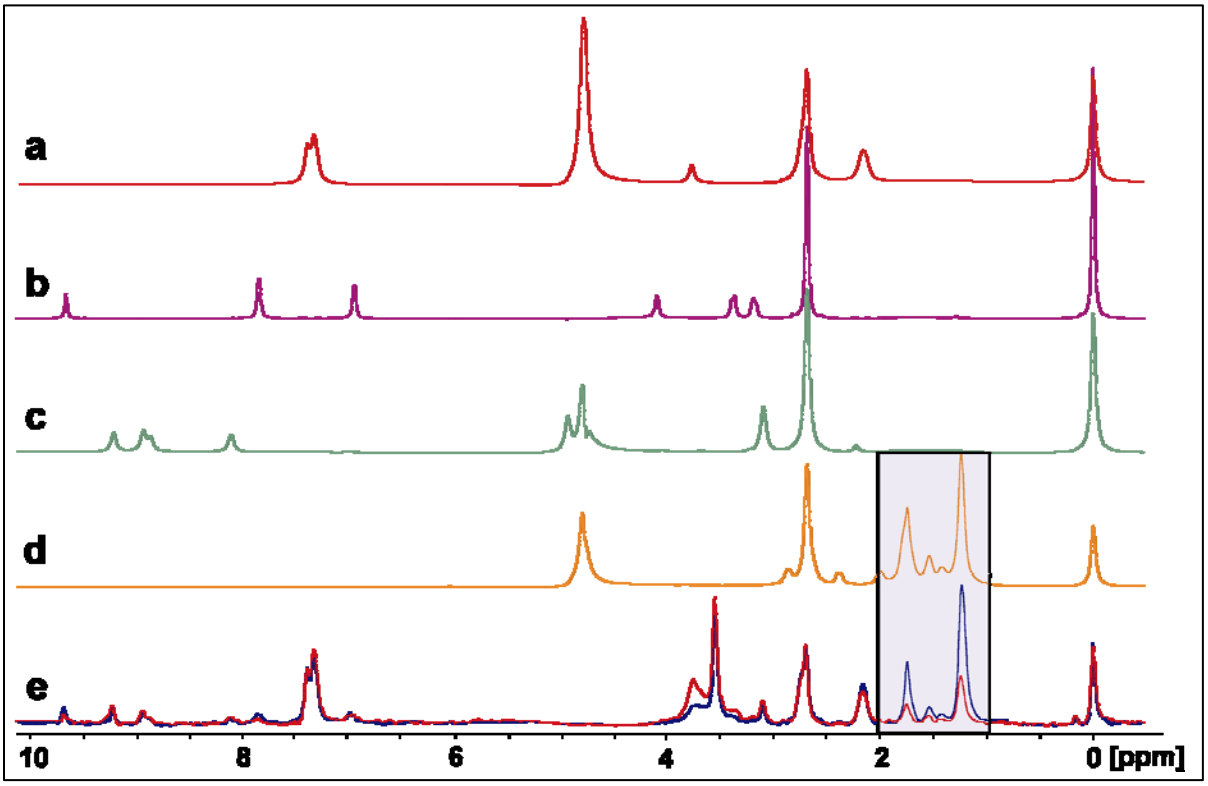

Figure 3. Detection of ligand binding to immobilized DsbB using TINS. The 1D ^{1}H NMR spectrum of 4 different fragments in solution (**a** - **d**) is shown for reference. The linewidths of the reference spectrum have been intentionally broadened to match those recorded in the presence of the sepharose support. The ^{1}H NMR spectrum of a mix of the 4 fragments in the presence of DsbB (**e**-red spectrum) or OmpA (**e**-blue spectrum) that have been immobilized on the sepharose support. The highlighted region shows the reduction in peak amplitude expected upon specific binding of a fragment to the immobilized target.

from Fourier transform and phasing to comparison of peak amplitudes and binder identification. The analysis was performed using in house written routines implemented in TopSpin, the spectrometer control and data analysis software. The screen resulted in 93 hits for DsbB, defined as fragments which had a TINS effect less than 0.3, as shown by an example of a mix containing a hit in Figure 3. This particular cut-off was chosen by virtue of a step-like relationship between the observed TINS effect and the number of "hits" whereby even slightly raising the cut-off gave a large increase (more than two fold) in the number of compounds that were selected as hits (not shown). The resulting hit rate for DsbB was 8.7 % which is well within the range we typically

observe with TINS (3 - 9.5 %). The higher hit rates of TINS with respect to other ligand based, NMR detected methods is readily explained by the sensitivity of TINS to binding as weak as 15 mM K_d, which is about 5 times lower than comparable screening assays. Application of the same criteria to OmpA binding identified 7 compounds as hits for a hit rate of 0.6 %, validating the earlier data suggesting that OmpA has minimal small molecule binding capacity and is therefore a good reference for membrane proteins.

Hit validation and characterization using enzymatic assays

Since the TINS assay simply identifies compounds that bind to DsbB, not necessarily hits which inhibit enzymatic activity, it is important to validate the hits in terms of biological activity. Enzyme inhibition studies using a single concentration (250 μM) were used to generate an initial ranking of the biological activity of the fragment hits (Figure 4). Each of the fragments identified as TINS hits was assayed for inhibition of DsbB-dependent reoxidation of DsbA. Compounds which interfered with the assay when run in either fluorescence or absorbance mode and were left out of the analysis. The remaining 74 hits exhibited a distribution of potencies against DsbB (Figure 4), including 60 % with better than 30 % enzymatic inhibition and 16 % with either less than 20 % inhibition or mild stimulation.

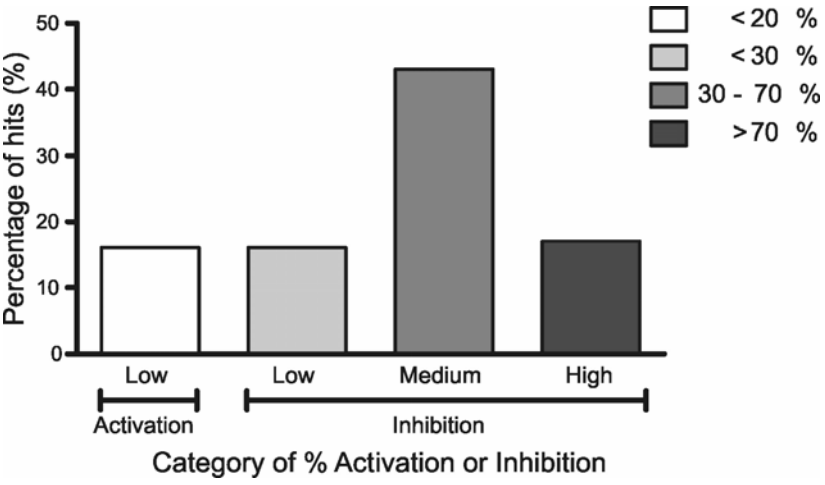

Figure 4. Distribution of biological activity of the hits found in the TINS fragment screen of DsbB. Each fragment was assayed singly at 250 μM.

a

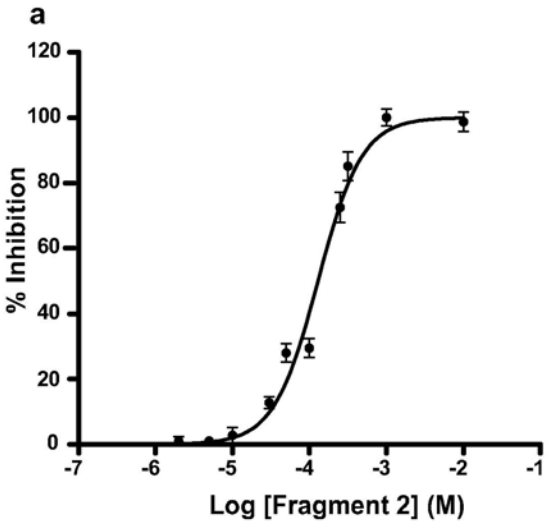

b

Fragment	IC50 (μM)	Hill coefficient
1	7 ± 1	0.80 ± 0.10
2	100 ± 10	1.40 ± 0.15
3	193 ± 11	1.20 ± 0.11
4	13 ± 1	0.80 ± 0.10
5	46 ± 12	0.80 ± 0.10
6	70 ± 10	1.00 ± 0.10
7	115 ± 11	1.15 ± 0.05
8	168 ± 10	1.40 ± 0.10

Figure 5. Potency determination for selected hits from the TINS screen. An example of an inhibition curve used to determine the IC_{50} (**a**). The curve represents the mean ± S.E.M. of three independent experiments performed in triplicate; (**b**) Inhibitory constants and Hill coefficients for the 8 most potent compounds.

The 13 fragments showing more than 70 % inhibition in the single concentration point assay were further analysed for potency (IC_{50}) by dose-response experiments (Figure 5). Dose response experiments were carried out with increasing fragment concentrations, from 0.0001 to 10 mM, while both DsbA and UQ1 were kept in excess. Three of the 13 fragments showed artefacts including signs of protein precipitation at higher compound concentration and/or steeper than expected Hill coefficients. The remaining 10 fragments titrated over 2 log orders and exhibited a Hill coefficient close to unity and are therefore well-behaved. The 8 most potent compounds had IC_{50} values between 7 and 200 μM and consisted of a variety of scaffolds (see Figure 6).

As an initial step towards delineating the molecular mechanism of DsbB inhibition, we carried out a more detailed kinetics analysis of the mode of action of the 8 most potent fragments. Substrate-velocity experiments were performed with either DsbA or UQ1 titrated in the presence of saturating amounts of the other. The titrations were then repeated in the presence of increasing amounts of the inhibitory fragment. There are several possible outcomes of such an experiment: a decrease in the apparent affinity for DsbA or for UQ1, in which case the fragment competes with

one of these for binding to DsbB, or mixed-model inhibition in which the apparent affinity for both decreases (Figure 6).

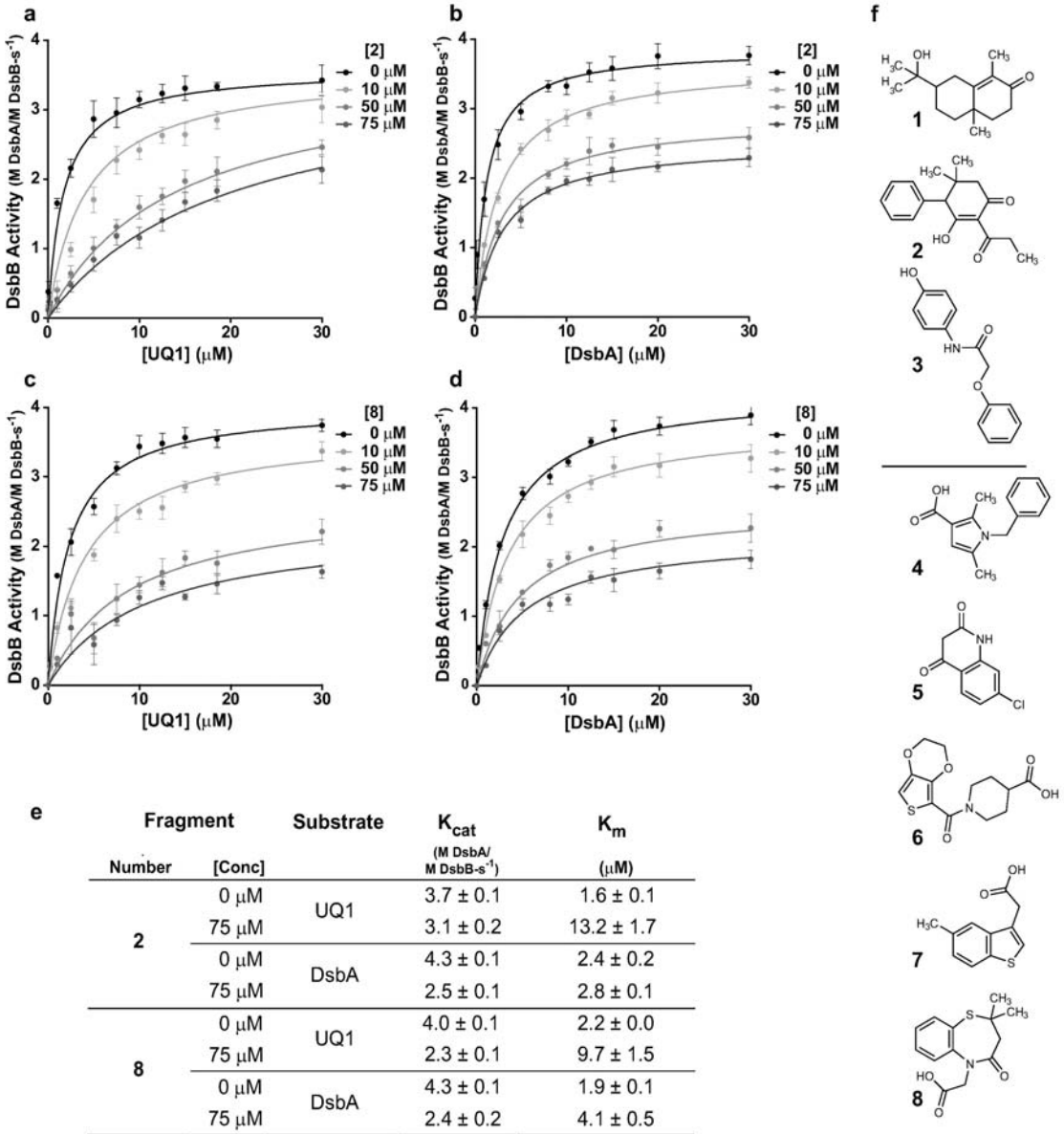

e

Fragment Number	[Conc]	Substrate	K_{cat} (M DsbA/ M DsbB-s^{-1})	K_m (μM)
2	0 μM	UQ1	3.7 ± 0.1	1.6 ± 0.1
	75 μM		3.1 ± 0.2	13.2 ± 1.7
	0 μM	DsbA	4.3 ± 0.1	2.4 ± 0.2
	75 μM		2.5 ± 0.1	2.8 ± 0.1
8	0 μM	UQ1	4.0 ± 0.1	2.2 ± 0.0
	75 μM		2.3 ± 0.1	9.7 ± 1.5
	0 μM	DsbA	4.3 ± 0.1	1.9 ± 0.1
	75 μM		2.4 ± 0.2	4.1 ± 0.5

Figure 6. Mode of action determination for the most potent DsbB inhibitors. Fragment **2** was assayed in competition with synthetic UQ1 (**a**), the electron acceptor, or DsbA (**b**) the electron source. Fragment **8** was assayed in the same manner (panels **c** and **d** respectively). The K_{cat} and K_m apparent determined from the data are shown in the table below (**e**) in the absence and presence of the indicated amount of each inhibitor. The structures of all 8 fragments are shown in **f**. The data indicates that fragments **1** – **3** are quinone competitive and fragments **4** – **8** are mixed mode inhibitors.

In this analysis, fragments **1 - 3** behaved similarly (Supplementary Figure 1). This group is exemplified by fragment **2** where increasing concentrations result in moderate perturbation of the maximum enzymatic turn over rate (K_{cat}) and apparent affinity of DsbA but a dramatic reduction (> 6 fold) in the apparent affinity of UQ1. This data suggests that fragments **1 - 3** compete for the same binding site as UQ1. On the other hand, addition of fragments **4 - 8** simultaneously decreased both the apparent affinity and the K_{cat} for Q1 and DsbA as best exemplified by fragment **8** (Figure 6 and Supplementary Figure 2). This data suggests a mixed model of inhibition of DsbB by these fragments. Mixed model inhibition could be explained if the fragments bound DsbB in such a way that limited access of both UQ1 and DsbA to their binding sites on DsbB. To investigate this possibility we sought 3D structural information on the binding site of the fragments.

Mapping of Fragment Binding on DsbB by NMR chemical shift perturbation

If the sequential assignment of a protein is available, analysis of chemical shift perturbation data affords rapid access to low resolution structural data to characterize ligand binding sites[28,236]. While the sequential assignment of wildtype DsbB is not available due to the poor quality of the NMR spectra, spectra of the DsbB[CSSC] double cysteine mutant are of high quality, resulting in a complete backbone resonance assignment for this form of the protein[62]. Accordingly, we titrated fragments **1 - 8** into ^{15}N labelled DsbB[CSSC] and acquired HSQC spectra at 1, 5 and 10 mM fragment concentrations. We titrated DMSO into ^{15}N DsbB[CSSC] to control for solvent induced chemical shift perturbations and subsequently a fragment was selected from the library that was scored as a non-binder in the TINS screen. As expected these titrations resulted in minimal shifts of peak positions, which were subsequently subtracted from the titrations of binding fragments. When purified from *E. coli,* DsbB[CSSC] contains the endogenous ubiquinone-8[99], thus compound specific for this site must compete with UQ-8 for binding. Synthetic UQ1 was titrated into a sample of ^{15}N DsbB[CSSC] to locate the resonances which were affected by *bona fide* binding to the ubiquinone site (Figure 8). We observed

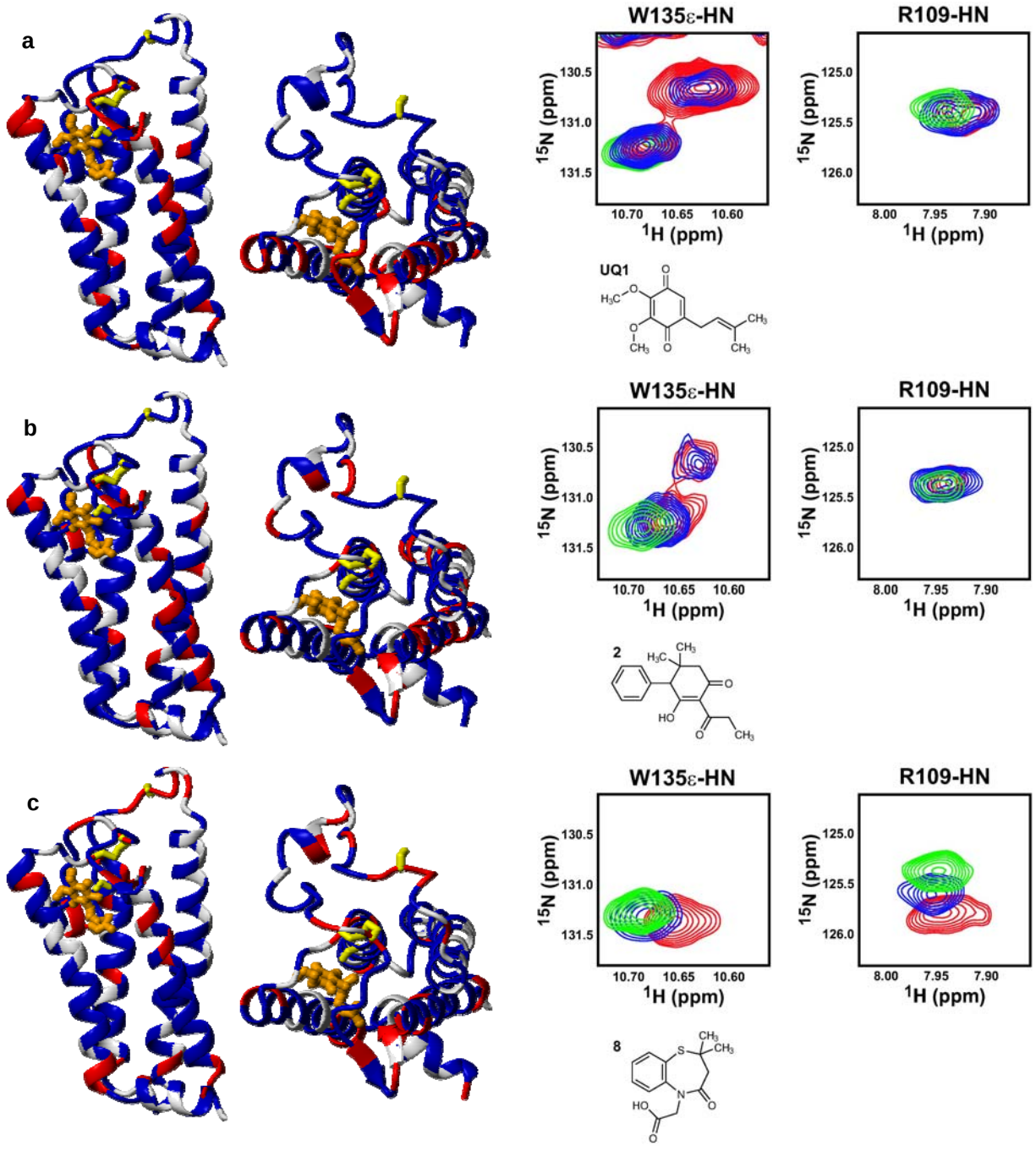

Figure 7: NMR analysis of fragment binding to DsbB. The 8 most potent fragments were titrated into ^{15}N DsbB[CSSC]. Data for the synthetic quinone UQ1 (**a**), competitive fragment **2** (**b**) and the mixed model fragment **8** (**c**) are shown.

Figure 7 (cont.): For each of these three compounds, the pattern of peak perturbations mapped onto the backbone structure, characteristic peak perturbations and the structure of the compound is shown. Residues with largest perturbations upon titration of the are indicated in red on the DsbB[CSSC] backbone structure (modified pdb ID 2k74[62]) viewed from the same orientation as in Figure 1 (left) and from the periplasmic face (right). The side chains of C41, S44, C104, and S130 are indicated in yellow. The coenzyme UQ2 (orange) is shown to indicate its binding site and the 23 unassigned residues from this study and 10 prolines are colored white.

significant chemical shift perturbations for a number of residues including the backbone amides of A22, Q33 and D136 as well as the sidechain indole of W135, all of which are in the areacorresponding to the endogenous quinone binding site, as reported previously in both the crystal and solution structures of DsbB[62,92]. In all cases, titration of UQ1 resulted in the appearance of peaks at a new chemical shift and the simultaneous disappearance of peaks from the spectrum of DsbB[CSSC] bound to endogenous quinone. This pattern of peak changes is indicative of slow exchange on the NMR time scale (e.g. k_{off} < 30 Hz $\Delta\delta$ in Figure 7), a fact that is not surprising given the similarity of UQ1 to other known synthetic substrates of DsbB (e.g. UQ2). The appearance of the UQ1 HSQC spectrum and the lack of visible protein precipitation indicate that the displacement of endogenous quinone by UQ1 is a reversible phenomenon that maintains the overall fold of the protein.

Addition of all 8 fragments to ^{15}N labelled DsbB[CSSC] resulted in readily detectable changes in chemical shifts, suggesting that the fragments selected by TINS screening and biochemical assays on wild type protein also bind the cysteine mutated form. The presence of chemical shift perturbations in solvent exposed loops as well as portions of the protein buried within the micelle suggests that the fragments were specifically binding to the protein and not non-specifically partitioning into the micelle. Fragments **1 – 3,** which competitively inhibited ubiquinone binding, induced chemical shift perturbations located on the first periplasmic loop, in close proximity to the active site cysteine Cys41 and the mutated residue Ser44. Unfortunately the key residue Arg48, previously identified as being involved in ubiquinone binding[92] could not be clearly assigned in our experiments, along with a few other residues in close proximity to the ubiquinone binding site (Figure 7). The pattern of chemical shift perturbations induced by this group, as best

exemplified by fragment **2**, closely resembles those induced by UQ1. First, titration of **2** into ^{15}N DsbB[CSSC] resulted in chemical shift changes in the same residues as for UQ1 and further, these changes suggested slow exchange. Similarly, R109HN, which is minimally affected by UQ1, undergoes only minor chemical shift perturbations in the presence of **2**. Further, mapping all of the chemical shift perturbations induced by **2** onto the backbone structure of DsbB[CSSC] reveals a pattern that strongly resembles that induced by UQ1 (compare Figure 7**a** to 7**b**).

In contrast, the chemical shift changes induced by fragments **4** – **8** differ in both the overall pattern and the details (Figure 7**c**). Addition of **8**, for example, to ^{15}N DsbB[CSSC] resulted in chemical shift perturbations in TM1 and TM2 close to the quinone binding site as with **2**, but additional extensive perturbations in the second periplasmic loop, especially the segment containing Cys104, involved in transferring electrons from DsbA to DsbB and the segment containing Pro100-Phe106, involved in DsbA binding[92]. Interestingly, the section containing the hydrophobic residues Leu116 and Val120, which are suggested to be involved in associating with the membrane during charge transfer from DsbA to DsbB[92], were affected by titration of fragments **4** - **8**, but not by Q1 or fragments **1** - **3**. Moreover, the details of the chemical shift perturbations differed significantly between fragments **4** - **8** and UQ1 or **1** - **3**. There was no evidence for slow exchange for any of the fragments **4** - **8**, although **4** & **7** show signs of line broadening of the backbone resonance of Q33 that may indicate intermediate exchange (not shown). Addition of **8** resulted in gradual, concentration dependent changes to W135ε NH that are indicative of rapid exchange while the position of the bound peak is very different from that in the UQ1 and **2** titrations. In contrast, the backbone amide of R109, which is only mildly perturbed by UQ1 or **2,** is very dramatically perturbed by the presence of **8**. This data suggests that fragments **4** - **8**, which exhibit mixed mode DsbB inhibition, bind in either a different mode or different site to fragments **1** - **3** which are competitive with ubiquinone.

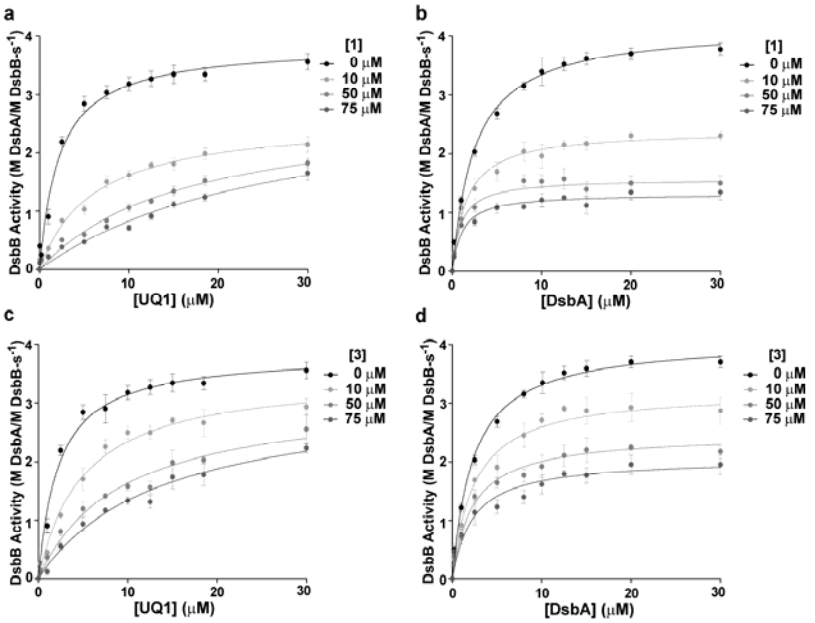

Supplementary Figure 1. Competition binding analysis of fragments showing UQ1-competitive inhibition of DsbB. The substrates UQ1 and DsbA were independently tested for competition by fragments **1** and **3**. In both cases, fragments showed competitive inhibition of UQ1 binding (**a**, **c**) and non-competitive inhibition of DsbA binding (**b**, **d**). The data is represented as the mean ± S.E.M. of three independent experiments performed in triplicates.

Fragment		Substrate	K_{cat} (M DsbA/ M DsbB-s^{-1})	K_m (μM)
No.	**[Conc]**			
1	0 μM	UQ1	3.8 ± 0.1	2.2 ± 0.2
	75 μM		3.7 ± 0.5	8.8 ± 0.4
	0 μM	DsbA	4.2 ± 0.2	2.5 ± 0.2
	75 μM		1.9 ± 0.5	2.3 ± 0,5
2	0 μM	UQ1	3.7 ± 0.1	1.6 ± 0.1
	75 μM		3.1 ± 0.2	13.2 ± 1.7
	0 μM	DsbA	4.3 ± 0.1	2.4 ± 0.2
	75 μM		2.5 ± 0.1	2.8 ± 0.1
3	0 uM	UQ1	3.8 ± 0,1	2,3 ± 0,2
	75 μM		2.9 ± 0.2	4.6 ± 0.2
	0 μM	DsbA	3.9 ± 0.1	2.3 ± 0.2
	75 μM		2.0 ± 0.5	3.2 ± 0.6

Supplementary Table 1. Summary of values for DsbB competition binding analysis graphically represented in Supplementary Figure 1. K_{cat} and K_m values for DsbB at 0 μM and 75 μM of fragments **1** to **3** are listed as the mean ± S.E.M. of three independent experiments performed in triplicates.

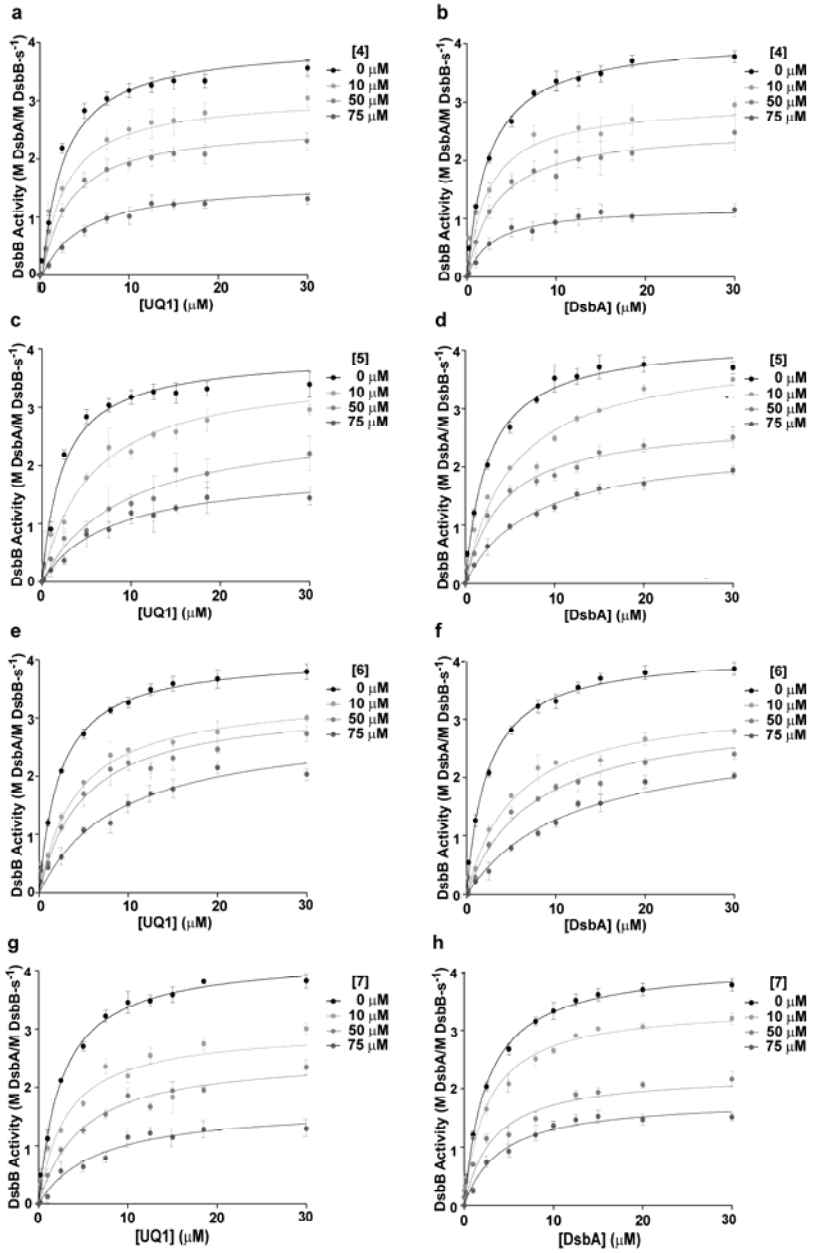

Supplementary Figure 2. Competition binding of fragments showing mixed model inhibition of DsbB. The substrates UQ1 and DsbA were independently tested for competition by fragments **4** to **7** and in all cases, fragments showed mixed model inhibition for UQ1 binding (**a**, **c**, **e**, **g**) and DsbA binding (**b**, **d**, **f**, **h**). The data is represented as the mean ± S.E.M. of three independent experiments performed in triplicates.

Fragment		Substrate	K_{cat} (M DsbA/ M DsbB-s^{-1})	K_m (μM)
No.	**[Conc]**			
4	0 μM	UQ1	3.9 ± 0.1	2.4 ± 0.2
	75 μM		1.6 ± 0.5	4.3 ± 0.6
	0 μM	DsbA	4.1 ± 0.2	2.2 ± 0.2
	75 μM		1.2 ± 0.1	3.0 ± 0.1
5	0 uM	UQ1	4.0 ± 0.1	2,4 ± 0,2
	75 μM		1.9 ± 0.1	6.3 ± 0,2
	0 μM	DsbA	4.2 ± 0.1	2.4 ± 0.2
	75 μM		2.3 ± 0.2	5.6 ± 0.1
6	0 μM	UQ1	4.0 ± 0.2	2.4 ± 0.4
	75 μM		3.6 ± 0.1	5.8 ± 0.3
	0 μM	DsbA	4.2 ± 0.4	2.3 ± 0.3
	75 μM		2.7 ± 0.5	7.8 ± 0.5
7	0 uM	UQ1	4.2 ± 0.0	2.5 ± 0.5
	75 μM		1.6 ± 0,1	5.9 ± 0.2
	0 μM	DsbA	4.1 ± 0.2	4.2 ± 0.5
	75 μM	DsbA	1.8 ± 0,3	5.9 ± 0.2
8	0 uM	UQ1	4.0 ± 0.1	2.2 ± 0.0
	75 μM		2.3 ± 0.1	9.7 ± 1.5
	0 μM	DsbA	4.3 ± 0.1	1.9 ± 0.1
	75 μM	DsbA	2.4 ± 0.2	4.1 ± 0.5

Supplementary Table 2. Summary of values for DsbB competition binding analysis graphically represented in Supplementary Figure 2. K_{cat} and K_m values for DsbB at 0 μM and 75 μM of fragments **4** to **8** are listed as the mean ± S.E.M. of three independent experiments performed in triplicates.

Discussion

The use of Ro3 compliant, so-called "drug fragments" as a starting point for drug discovery, in combination with 3D structural information of target-fragment complexes, has delivered a number of innovative compounds which are currently in clinical trials[21]. However, this success has so far been strictly limited to soluble, moderately sized protein targets. Membrane proteins have not made good targets for FBDD due to their challenging physicochemical properties. In particular, the difficulty of generating sufficient quantities of purified, functional protein and of detecting specific binding to the target, as opposed to non-specific partitioning into hydrophobic phases, have limited the applicability of biophysical ligand screening approaches. Here we have addressed these two issues by a) immobilizing the target and reusing a single sample to screen an entire fragment collection and b) using a reference sample to cancel out non-specific interaction of the fragments with the hydrophobic phase. An additional, likely important, factor contributing to the low false positive rate is that the fragments that make up the collection are highly soluble, with each having been tested at 500 μM in an aqueous buffer alone and in a mixture. Using our Target Immobilized NMR Screening approach we have screened a collection of nearly 1,100 fragments with a single sample of less than 2 mg of protein and found 93 ligands. A number of observations suggest that these fragments are directly binding to DsbB and not indirectly *via* the micelle. First, there is a range of potencies in the enzyme inhibition studies that includes a small number of non-inhibitors and activators. Second, and perhaps more critically, inhibition is saturable and occurs over 2 log orders, strongly suggesting a stoichiometric interaction. Third, titration of 8 different fragments into ^{15}N labelled DsbB resulted in chemical shift perturbations at well defined sites in both solvent exposed and micelle buried portions of the protein. In particular, the similarity of the chemical shift perturbations induced by the synthetic quinone UQ1 and fragment **2** indicate the compounds are binding to the same site.

The eight fragments with greatest potency in the single concentration enzyme inhibition assay were fully characterized for potency, mode of action, and binding site on DsbB. This analysis suggests that these fragments can be divided into two groups, one that competes only with

quinone for DsbB binding and a second that perturbs the apparent affinity of DsbB for both quinone and DsbA. The clearest examples of the different behaviour are fragment **2**, which is quinone competitive and fragment **8** which exhibits mixed mode inhibition. The difference is best exhibited by the differing effect on the apparent K_m for UQ1 or DsbA that these two compounds have. While addition of fragment **2** at 75 μM reduced K_m for UQ1 more than 8-fold, it had only a marginal effect on the K_m for DsbA (only 5 % greater than experimental error). In contrast, addition of **8** at 75 μM reduced K_m for UQ1 more than 4.4-fold and K_m for DsbA more than 2-fold.

Titration of fragments **2** and **8** into ^{15}N labelled DsbB[CSSC] further supports a different mechanism of action of these two inhibitors. The differences can be most clearly seen by concentrating on the resonances from the backbone amide of R109 and the sidechain indole of W135. Titration of UQ1 into ^{15}N labelled DsbB results in the simultaneous appearance of a new peak at a nearby position and the reduction of the peak from W135ε NḤ from the endogenous quinone bound form. Since the other indoles are largely unaffected, we have tentatively assigned the new peak to W135ε NH in the UQ1 bound form. Addition of **2** resulted in concentration dependent shifts in the position of W135ε NH and the simultaneous disappearance and appearance of a new peak, as with UQ1. This new peak has an almost identical chemical shift (^1H & ^{15}N) as the UQ1 bound form. This behavior is consistent with two processes occurring. The first is a competition between **2** and the quinone moiety of the bound UQ8, consistent with the competitive kinetics observed for this inhibitor. However, we have shown that the isoprenyl tail of UQ8 extends down the groove between TM1 and TM4, making extensive interactions with the protein. Therefore, displacement of the quinone moiety likely does not immediately result in dissociation of UQ8 from DsbB[CSSC]. Apparently, this occurs on a slower timescale, resulting in the observation of a new peak with a quite different chemical shift. Addition of **8** to ^{15}N labelled DsbB[CSSC] also causes chemical shift perturbation of the W135ε NḤbut these are exclusively concentration dependent and the bound state has a different resonance frequency than the bound state of UQ1 or **2**. Also, addition of **8** causes a large downfield shift in the resonance of R109N that is concentration dependent while UQ1 and **2** had no or only minor effects on this peak.

When the chemical shift perturbations are plotted on the structure of DsbB[CSSC], a distinct difference is observed between UQ1 and **2** on the one hand, and **8** on the other. UQ1 and **2** induce similar shift perturbations which are primarily located in TM 1, 2 and 4. Fragment **8** induces fewer and smaller shifts which are primarily in the periplasmic end of TM1 and 4, but significantly more and larger shifts in both PL2 and PL2'. We propose a simple structural model that is consistent with the results of the biochemical mode of action study and the chemical shift perturbation analysis. In this model, the quinone competitive fragments **1** - **3**, bind directly in the quinone binding pocket and displace the endogenous quinone. In contrast, the mixed mode fragments **4** - **8** bind on the periplasmic side of the ubiquinone binding site in the immediate neighbourhood of PL2' and do not displace endogenous ubiquinone. This binding site would both reduce electron transfer to the ubiquinone and perturb the conformation of the periplasmic loops that form the binding site for DsbA, thereby reducing the binding affinity of DsbA.

We note that the concentration of the fragments required to induce chemical shift perturbations in DsbB[CSSC] is significantly higher than the IC_{50} values measured for the wild type protein. In addition, UQ1 dependent chemical shift perturbations occurred in the same concentration range as the fragments. A likely explanation is that the conformation of the mutant differs slightly from the wild type protein, against which the fragments were selected. In addition, either the affinity for the quinone is higher for the DsbB[CSSC] mutant or more likely, the quinone binding site may be partially occluded. This latter possibility is clearly consistent with the reduced dynamic behaviour of DsbB[CSSC] with respect to the wild type protein, which results in the substantial improvement in the quality of the NMR spectra. This reduced dynamic behaviour of the disulfide mutant may be responsible for the slow exchange kinetics observed for UQ1 and **2** if release of the ligand from this binding site (endogenous ubiquinone, UQ1 or **2**) can only occur from a sparsely populated conformation.

Since TINS does not require any specific characteristics of DsbB, it should, in principle, be broadly applicable for fragment discovery with membrane proteins. Although the present study used deuterated detergent, this is not *a priori* a requirement. Many detergents that are compatible with membrane proteins have lower CMC values than DPC and therefore could be used at much lower concentration. Since the detergent would be at least 10 fold lower in concentration than the

compounds, its NMR signals would not interfere with the aliphatic signals of the compounds, while aromatic signals would occur in an entirely different portion of the spectrum. Furthermore, non-detergent media for solubilizing membrane proteins have been developed that are more compatible with protein function. These media, such as nanodiscs[68,73,74] and amphipols[72,180,181], are compatible with most membrane proteins and should prove highly complementary to the TINS technology for finding fragments that bind membrane proteins, as can be seen in Chapter 6.